The 2012 World Congress on
Advances in Civil, Environmental, and Materials Research (ACEM' 12)
Seoul, Korea, August 26-30, 2012

CFD simulation of wave and current on fixed cylinder

T.J. Kang*, Y.H. Park*, W.G. Park‡

School of Mechanical Engineering, Pusan National University, Busan 609-735, Korea

J.K. Cho**

Research Institute for Future Wind Energy Technology, Pusan National University, Busan 609-7 35, Korea

Abstract. In the present study, CFD simulation is performed for wave and current on 3D fixed cylinder. In order to simulate 3D incompressible viscous flow in a numerical wave tank with cylinder, the present study used ANSYS FLUENT based on the finite volume method. Volume-Of-Fluid(VOF) scheme is used to capture two phase interface,. In the numerical wave tank, wave maker is controlled by inlet boundary condition using Airy wave theory. Also, outgoing wave is dissipated in an artificial damping zone at the end of the tank. First of all, characteristics of wave are inspected to varying the wave length and amplitude. In addition, a fixed cylinder is calculated with wave and uniform current. Increment and computed wave amplitude slightly differ increasing wave steepness. And the computed results represent that wave force increases as Froude number increases

Key words: Regular wave, Wave absorber, Froude number, Cylindrical cylinder, Airy wave theory, Vertical force, Run-up elevation

1. Introduction

Recently, the necessity of the use of clean and renewable energy resources has been highlighted highly due to the limitation of the fossil energy and the increment of the environmental pollution. The research on the clean and renewable energy resources such as wind power energy is the key subject of the alternative energy development. With the developments of the design technique and increment of energy demand, the wind turbine rotor is enlarged gradually. Therefore installation area is being extended into the deep sea that wind energy resource in rich more than the on the shore.

One of the main roles of wind turbine substructure is to support and control the wind turbine generator. But due to complex wave, current and marine environment in the deep sea, it is required that design technique is more precise. To obtain better design techniques, it is necessarily required to load analysis including flow analysis.

Substructure is studied by many researchers. The horizontal fixed cylinder was experimentally examined by Dixon(1979) with change of Progressive regular wave. Using same geometry and wave condition, Westphalen(2009) and Jonas(2011) is numerically studied with comparison of experimental results(Dixon, 1979). Vennugopal(2009) was experimentally examined drag and inertia coefficient for rectangular cylinder with changes of aspect ratio. For the vertical fixed cylinder , Mercier(1994) was experimentally examined. Using same model, Park(1999) and Celebi(2001) were numerically

‡ Professor, corresponding author, *E-mail*: wgpark@pusan.ac.kr
** Research Professor
* Graduate Student

studied 1,2,3 order hormone for wave elevation. Also, Influence of Current velocity was studied by change of Froude number. Leen(2007) was investigated wave run-up for various wave conditions(steepness, height, depth. Boo(2006) was experimentally studied for higher harmonic wave force, it was compared to FNS(Faltisen-Newman-Vinje) model. Park(2011) was studied force acting on the substructure for wave and current. And then, the computed results were compared to experimental and analytic results(Morison equation).

In the present study, a 2D numerical wave tank was constructed to generate progressive regular wave. And then, these results were compared to progressive regular wave with change of current velocity. With expansion in 3D, the horizontal and vertical fixed cylinder were studied run up elevation and load acting on substructure with change of wave and current.

2. Description of 2D Numerical Wave Tank

Prior to analysis of fixed cylinder, a 2D numerical wave tank was constructed to generate progressive regular wave.

2.1 Geometry and boundary conditions

Wave condition and geometry of Numerical wave tank used in the present study is same to numerical wave tank used by Park(2011). The horizontal length is 7-meter, the vertical length is 3m. Water depth is 2m, Height of air region above free surface is 1m. Computational domain is discretizated to structured grid. Grid number is approximately 110,000 as 520 x 214. To capture the free surface accurately, grid is clustered near free surface. In the wave absorption region, grid is set up 20 grids to horizontal direction. Grid of the wave absorption region was used to generate numerical diffusion obtained by grid clustering(Fig. 1). Generation of geometry and grid were used to GAMBIT as commercial pre-processor program. Fig. 1 shows computational domain. For generation of progressive regular waves, wave maker was used to velocity profile at inlet in the current study. This velocity profile is obtained by Airy's wave theory(Robert and Robert, 1991). Bottom is assumed to slip wall, boundary condition of air region was prescribed to atmosphere pressure. Outlet of water region was prescribed to hydrostatic pressure. The velocity profile used in inlet is as follows:

$$u = A\omega \frac{\cosh k(y+d)}{\sinh kd} \cos(\mathrm{kx} - \omega\mathrm{t}) \tag{1}$$

$$v = A\omega \frac{\sinh k(y+d)}{\sinh kd} \sin(\mathrm{kx} - \omega\mathrm{t}) \tag{2}$$

Where A is wave amplitude, ω is circular frequency, d is wave depth, k is wave number.

Dissipation zone is far from 2m at outlet(Fig. 1). Adding the following formula (3) in the momentum source, momentum of wave was dissipated.

$$S = -C\left(\frac{1}{2}\rho|V|V\right)\left(\frac{x-x_s}{x_e-x_s}\right)^2\left(\frac{y_b-y}{y_b-y_{fs}}\right) \tag{3}$$

Where ρ is water density, V is velocity magnitude. The subscripts s and e denote the start and end positions of dissipation zone in the x-direction, respectively, and b and fs denote the bottom and free surface positions of the dissipation zone in the z-direction, respectively. C is user-defined empirical coefficient, it was set up 10 in the present study. In the present study, velocity profile, hydrostatic pressure, momentum source for dissipation zone were used to UDF(User Define Function) provided by ANSYS FLUENT. The above information is provided in FLUENT manual(Fluent, 2010).

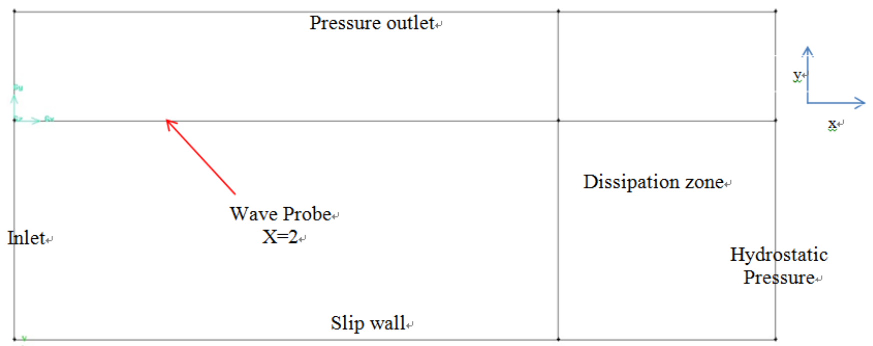

Fig. 1. Computational Domain and boundary condition

2.2 Numerical method

The CFD calculations shown here are based on simulated solutions to the incompressible Navier-Stokes equation, carried out using ANSYS FLUENT v.13. Volume-Of-Fluid(VOF) method is used to capture two phase interface. Pressure-velocity coupling for incompressible flow is used to SIMPLE(Semi-Implicit Method for Pressure-Linked Equations). This method denotes Patankar(1972). Momentum discretization is QUICK(Quadratic Upwind Interpolation for Convection Kinetics) scheme. Discretization of volume of fraction is used to Geo-Reconstruct(Fluent, 2011).

2.3 Parametric study for numerical wave tank

To verify numerical wave tank, parametric study was conducted with change of wave period, wave amplitude. And then, this result is used to verify designed waveform for the space and time. Table 1 show wave profile used in the parametric study. Wave profile used in the present study refer to Park(2011). Position of wave probe is far 2m from horizontal direction in the inlet. At the position Volume of fraction is 0.5, the position of the free surface is determined.

Table 1 Condition of wave profile

Period(T)	Amplitude(A)	Steepness(H/L)
0.6	0.03	0.11
0.8	0.05	0.1
	0.04	0.08
	0.03	0.06
1.0	0.03	0.04
1.2	0.03	0.03

Where H is wave height, L is wave length.

Fig. 2 show wave elevation and volume fraction(air) for the space. In x=5~7m adopted the wave absorber, Fig. 2 show wave amplitude to decline suddenly.

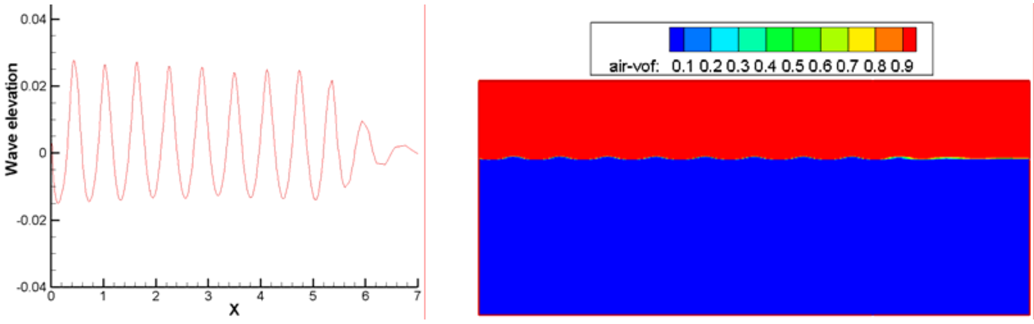

Fig. 2. Spatial profile and Volume fraction(air) of regular wave at wave period=0.8s

Fig. 3 show variation of wave elevation with change of wave period or wave amplitude. When incident wave amplitude is fixed to 0.03m, Fig. 3(a) show variation of wave elevation at T=0.6, 0.8, 1.0, 1.2(s). Also, when incident wave period is fixed to 0.8s, Fig. 3(b) show variation of wave elevation at A=0.03, 0.04, 0.05(m). According to Fig 3(a),(b), wave period represents good agreement with incident wave period. But wave amplitude has a few difference compared to incident wave amplitude. Fig 3 show that wave amplitude is less than incident wave amplitude as wave steepness increases. This is due to phenomenon of wave breaking generated at inlet(wave maker) when wave steepness is relatively high(Park, 2011).

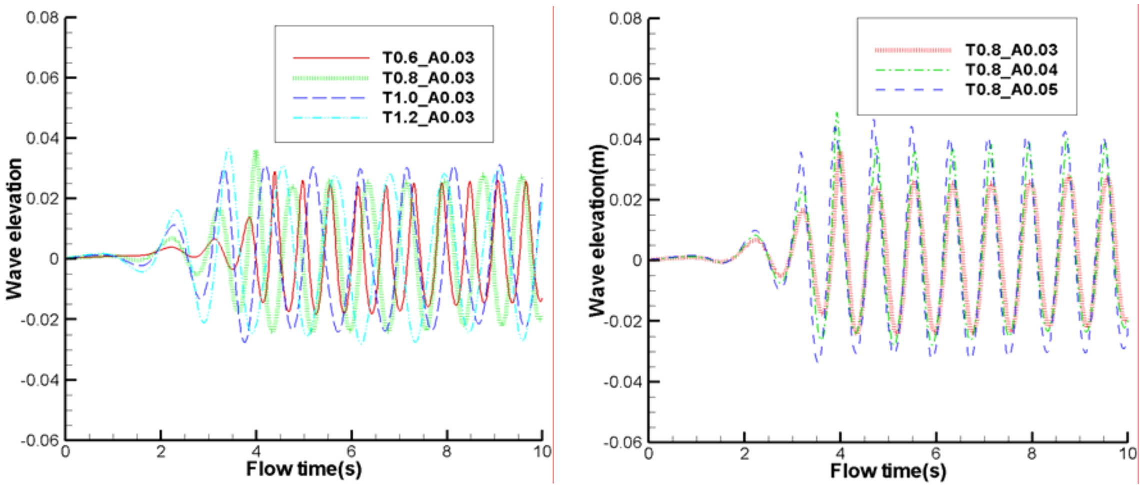

(a) Wave amplitude=0.03m (b) Wave period=0.8s

Fig. 3. Time history of wave elevation at x=2m

Next, study is investigated interactions between wave and current. Robert(1991) modifies Airy's wave theory with uniform current velocity is given by

$$\omega = V_c k + \sqrt{gk \tanh(kd)} \tag{4}$$

$$\phi = -V_c k + B \cosh k(d+z) \cos(kx - \omega t) \tag{5}$$

$$B = \frac{gH}{2\omega(1 - V_c / C)\cosh(kd)} \tag{6}$$

Where V_c is current velocity, ϕ is velocity potential, C is wave speed. When V_c is 0, formula (4)~(6) become Airy's wave theory without current. Fig. 4 show wave elevation with change of current velocity. Where current velocity represent using Froude number, $F_r = V_c / \sqrt{gd}$. As increase Froude number wave amplitude increase and wave period decrease in the current study.

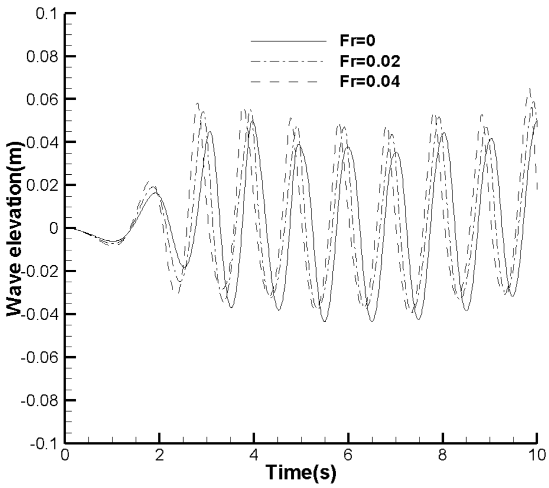

Fig. 4. Time history of wave elevation at x=2m with change of current velocity

3. Study for fixed cylindrical substructure with numerical wave tank

3.1 Analysis of horizontal fixed cylinder with change of wave condition

First of all, a horizontal fixed cylinder is investigated for change of wave condition in the present study. The computed results is compared to experimental results performed by Dixon(1979). Specification of numerical wave tank in the present study is as below. The horizontal length is 6-meter, the vertical length is 1.8m. Water depth is 0.9m, Height of air region above free surface is 0.9m. Diameter of horizontal fixed cylinder is 0.1m and transverse length is 1m. Table 2 shows wave profile used in the current study.

Table 2 Condition of wave profile

Period(T)	Amplitude(A)	Steepness(H/L)
0.9597	0.05	0.067
0.9775	0.02	0.027
0.9728	0.03	0.04

A relative wave force is computed with change of cylinder depth below free surface. A relative wave force is defined by

$$F' = \frac{F}{\rho g\left(\frac{\pi D^2 l}{4}\right)} \tag{7}$$

Where F, l, ρ, g, D represent vertical force, transvers length, water density, acceleration of gravity, and diameter of cylinder, respectively. Fig. 5 show free surface with change of cylinder depth. In the present study, cylinder depth are 0, 0.03, 0.06m.

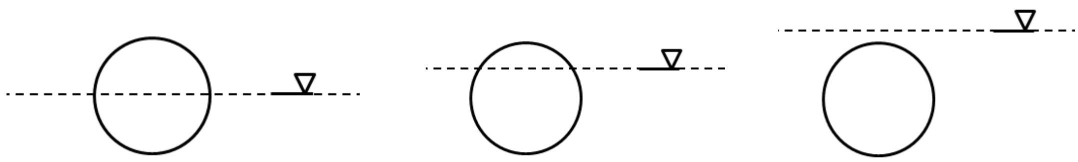

(a) d'=0 (b) d'=0.03 (c) d'=0.06

Fig. 5. Cylinder depth(d') for the three simulations

Fig. 6 show computational domain including boundary condition. Boundary condition of 3-dimension is same to 2-dimension. Computational domain is discretizated to structured grid. Grid number is approximately 440,000 . To capture the free surface accurately, grid is clustered near free surface.

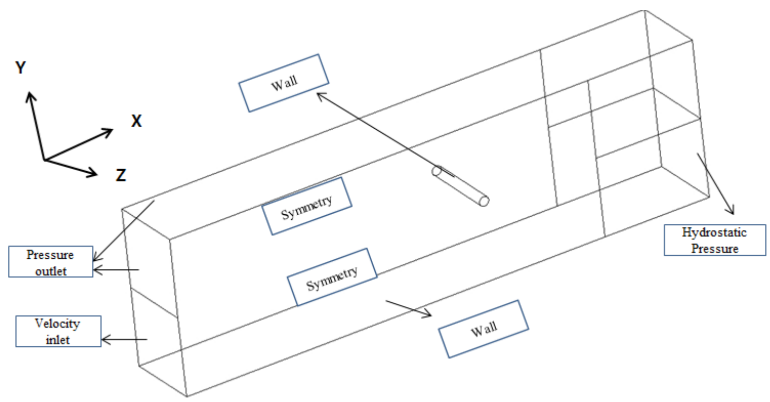

Fig. 6. Computational Domain

Fig. 7 show relative vertical force for 1 period with change of cylinder depth. Physical time of computed results is approximately 10 seconds. The results represented good agreement with the experimental results. But when wave elevation is crest(T=0.73), the computed results represent slightly higher than the experimental results. Fig. 8 represents surface profile of cylinder for d'=0. In d'=0, wave amplitude and radius of cylinder is 0.05m. Therefore when wave elevation is though, the cylinder must be not submerged for free surface. But, the current results shows that the cylinder is slightly submerged at T=0.73. This disagreement appears because the wave amplitude of current results is slightly higher than incident wave amplitude at though.

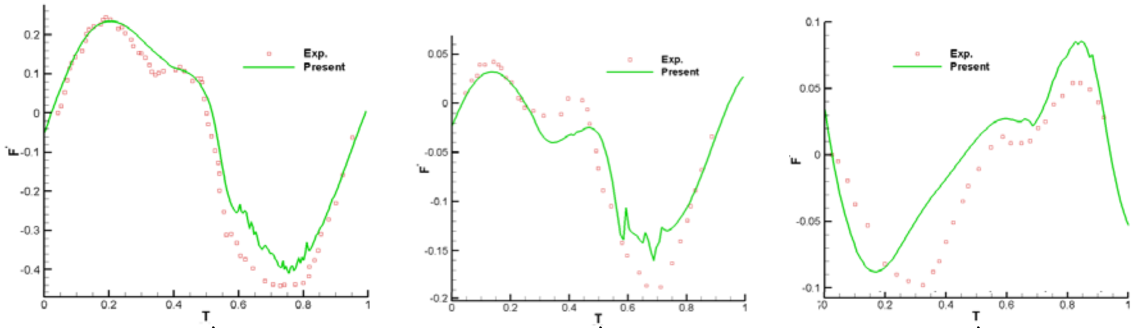

(a) d'=0 (b) d'=0.03 (c) d'=0.06

Fig. 7. Vertical force with change of cylinder depth(d')

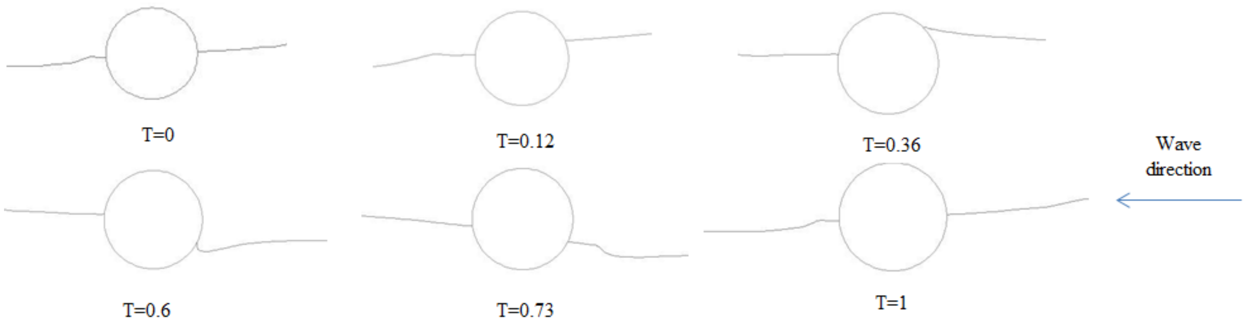

Fig. 8. Surface profile around the cylinder for d'=0

3.2 Analysis of vertical fixed cylinder with change of wave and current

Second, a vertical fixed cylinder is investigated for change of wave and current in the present study. The computed results is compared to experimental results performed by Kriebel(1992). Specification of numerical wave tank in the present study is as below. The horizontal length is 12-meter, the vertical length is 1.8m. Water depth is 0.9m, Height of air region above free surface is 0.9m. Diameter of horizontal fixed cylinder is 0.325m and vertical length is 1.8m. Table 3 shows wave profile used in the current study. The wave period and length is obtained by dispersion relation that is assumed intermediate depth wave as kd=1.332(Robert, 1991). The wave length is obtained by incremental-search method.

Table 3 Condition of wave profile

ka	Kd	kH
0.481	1.332	0.186
		0.317

In the current study, a Run-up elevation of the wall is investigated by the computed results. Fig. 9 represents run-up position with change of angle.

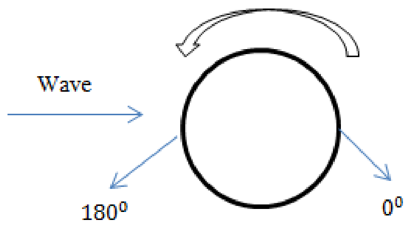

Fig. 9. Convention of run-up angle

Fig. 10 show run-up elevation with change of run-up angle(α_R) at kH=0.186, 0.372. Where R is run-up elevation. The run-up elevation is obtained by average of run-up elevations between 0~20 second. The computed results are not similar to the experimental results at α_R=180^0. A non-linearity generated by interaction between substructure and wave causes these results. Also, this disagreement appears because the wave amplitude of current results is slightly lower than incident wave amplitude at crest. But next study is conducted influence on current and wave because computed and experimental results are represented for similar tendency.

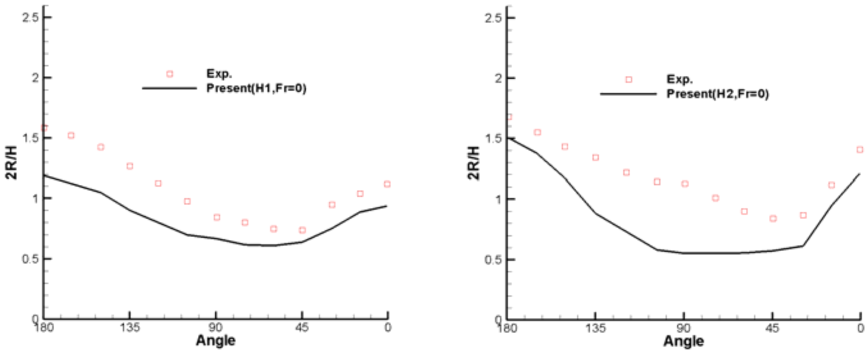

(a) kH=0.186 (b) kH=0.372

Fig. 10. Run-up elevation with change of run-up angle at kH=0.186, 0.372

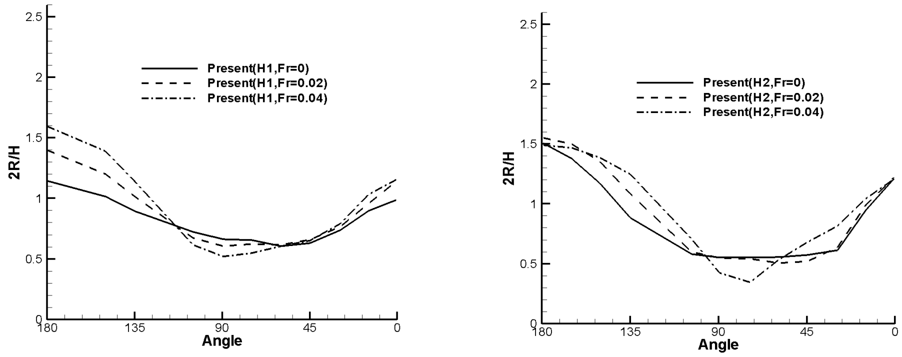

(a) kH=0.186 (b) kH=0.372

Fig. 11. Run-up elevation with change of run-up angle and current velocity at kH=0.186, 0.372

Fig. 11 represents run-up elevation with change of current velocity at kH=0.186, 0.372. Totally, As increase Froude number run-up elevation increase except for approximately $\alpha_R=60^0\sim105^0$. The non-linearity of substructure cause low run-up elevation at $\alpha_R=60^0\sim105^0$. Lower run-up elevation at $\alpha_R=60^0\sim105^0$ represent because as increase Froude number run-up elevation increase.

Next, horizontal wave force of the cylinder is investigated with change of Froude number. A wave force(F) is defined by

$$F = \frac{F_x}{\rho g A r^2} \tag{8}$$

Where F_x represent horizontal force.

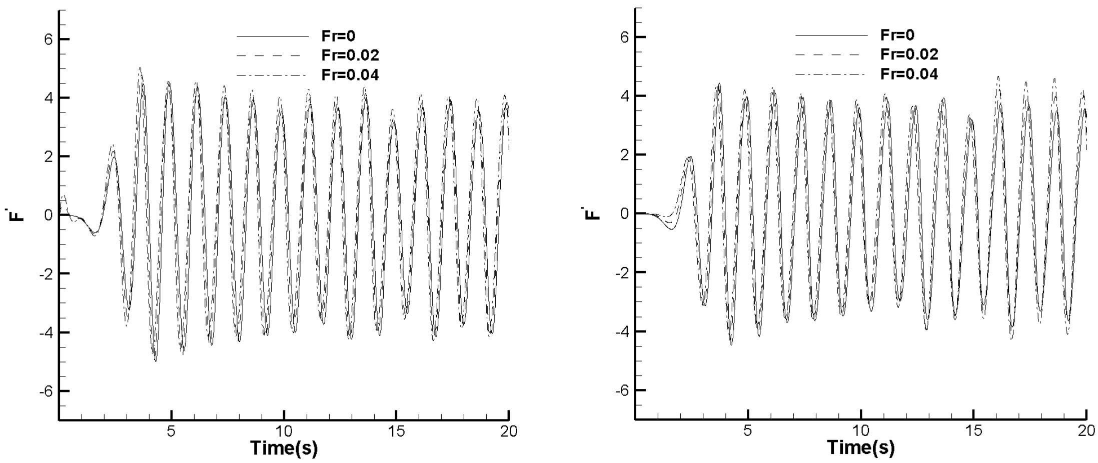

(a) kH=0.186 (b) kH=0.372

Fig. 12. Time history of horizontal wave force at kH=0.186, 0.372

Fig. 12 represents that horizontal force increases as Froude number increases. These results are similar to tendency of wave elevation with change of Froude number as shown in figure 4.

5. Conclusion

In the present study, wave force and elevation of the fixed cylinder is investigated to design complex wind turbine substructure with change of wave, current. Horizontal and vertical cylinder is used in the present study. The computed results are compare to experimental results. And then, study is conducted influence on current. For horizontal cylinder, vertical wave force is significantly predicted at though. This disagreement appears because the wave amplitude of current results is slightly higher than incident wave amplitude at though. Also, the run-up elevation of the vertical cylinder is under-predicted experimental results. This disagreement appears because the wave amplitude of current results is slightly lower than incident wave amplitude at crest. And the computed result of vertical cylinder represents that horizontal force increases as Froude number increases. These results are similar to tendency of wave elevation with change of Froude number

Acknowledgement

This work was supported by the New & Renewable Energy of the Korea Institute of Energy Technology Evaluation and Planning(KETEP) grant funded by the Korea government Ministry of Knowledge Economy (No. 20113020020010).

References

ANSYS FLUENT User's Guide, 2010.

Bai, W., Taylor, R.E. (2009), "Fully nonlinear simulation of wave interaction with fixed and floating flared structures", *Ocean Engineering.,* Vol. 36., pp. 223-236.

Boo, S.Y. (2006), "Measurements of higher harmonic wave forces on a vertical truncated circular cylinder", *Ocean Engineering.,* Vol. 33., pp. 219-233.

Celebi, M.S. (2001), "Nonlinear transient wave-body interactions in steady uniform currents," *Computer methods in applied mechanics and engineering*, Vol. 190(39), pp. 5149-5172.

Dixon, A.G., Greated, C.A., Salter, S.H. (1979), "Wave Forces on Partially Submerged Cylinders", *Journal of the Waterway Port Coastal and Ocean Division.,* Vol. 105(5)., pp. 421-438.

Jonas, A. (2011), *Simulation of Wave Induced Forces on Semi Submerged Horizontal Cylinders Using OpenFOAM*, CHALMERS University of technology, Master's Thesis, Goteborg, Sweden.

Kriebel, D.L., (1992), "Nonlinear wave interaction with a vertical circular cylinder. Part 2", Ocean engineering, Vol. 19, pp. 75-99.

Leen, D.V., Peter, F., Julien, D.R. (2007), "Wave run-up on cylindrical and cone shaped foundations for offshore wind turbines", *Coastal Engineering.,* Vol. 54., pp. 17-29.

Mercier, R.S., Niedzwecki, J.M. (1994), "Experimental measurement of second-order diffraction by a truncated vertical cylinder in monochromatic waves", *Proceedings of the 7th International conference Behavior of Offshore Structures.*, pp. 265-287.

Park, Y.S., Chen, Z.S., Kim, W.J. (2011), "CFD Application to Evaluation of Wave and Current Loads on Fixed Cylindrical Substructure for Ocean Wind Turbine," *Journal of Ocean Engineering and Technology.*, Vol. 25(2)., pp. 7-14.

Park, J.C., Kim, M.H., Hideaki, M. (1999), "Fully non-linear free-surface simulations by a 3D viscous numerical wave tank," *int J Numer Meth Fluids*, Vol. 29, pp. 685-703.

Patankar, S.V., Spalding, D.B. (1972), "A Calculation Procedure for Heat, Mass and Momentum Transfer in Three-Dimensional Parabolic Flows", Int. J. Heat Mass Transfer, Vol. 15, pp. 1787.

Robert, G.D. and Robert, A.D. (1991), *Water wave mechanics for engineers and scientists*, World Scientific.

Sumer, B.M. and Jorgen, F. (2006), *Hydrodynamics around cylindrical structures*, World Scientific.

Venugopal, V., Varyani, K.S., Westlake, P.C. (2009), "Drag and inertia coefficients for horizontally submerged rectangular cylinders in waves and currents", *Proceedings of IMechE Vol. 223 Part M: J. Engineering for the Maritime Environment*.

Westphalen, J., Greaves, D.M., Williams, C.K., Taylor, P.H., Causon, D.M., Mingham, C.G., Hu, Z.Z., Stansby, P.K., Rogers, B.D., Omidvar, P. (2009), "Extreme Wave Loading on Offshore Wave Energy Devices using CFD: a Hierarchical Team Approach", *Proceedings of the 8th European Wave and Tidal Energy Conference,* Uppsala, Sweden.